Carrier concentration independent antiferromagnetic spin fluctuations in the electron-doped high-temperature superconducting cuprate $Pr_{2-x}Ce_xCuO_4$

G. V. M. Williams,[1,2] S. Krämer,[1,*] R. Dupree,[3] and A. Howes[3]
[1]*2. Physikalisches Institut, Universität Stuttgart, D-70550 Stuttgart, Germany*
[2]*Industrial Research, P.O. Box 31310, Lower Hutt, New Zealand and MacDairmid Institute for Advanced Materials and Nanotechnology, Victoria University, Private Bag, Wellington, New Zealand*
[3]*Department of Physics, University of Warwick, Coventry CV4 7AL, United Kingdom*
(Received 28 August 2003; published 12 April 2004)

We have performed ^{63}Cu NMR measurements on the electron-doped high-temperature superconducting cuprate (HTSC) $Pr_{2-x}Ce_xCuO_4$ ($x=0.10$, 0.15, and 0.20), at 9 T, which is sufficient to suppress T_c to zero. The Cu spin-lattice relaxation rate and the Cu spin-lattice relaxation rate anisotropy can be consistently interpreted in terms of coupling to antiferromagnetic spin fluctuations for temperatures as low as 6 K. We find that the spin-fluctuation spectrum probed by the Cu spin-lattice relaxation rate does not change with increasing electronic concentration, contrary to a recent theoretical predication. There is no evidence in the Cu spin-lattice relaxation rate data for a temperature-independent spin gap that is as large as theoretically predicted or as large as the normal-state pseudogap energy reported from infrared reflectance measurements on the electron-doped HTSC $Nd_{2-x}Ce_xCuO_4$. The Cu nuclear quadrupole resonance frequency is significantly smaller than that observed in the hole doped HTSC, which implies a nearly complete cancellation of the Cu $3d$, O $2p$, and nuclei contributions to the electric-field gradient at the Cu nucleus. The orbital shift anisotropy is similar to that observed in the hole doped HTSC, implying a similar relative splitting of the Cu $3d$ orbitals.

DOI: 10.1103/PhysRevB.69.134504 PACS number(s): 74.72.Jt, 74.25.Nf, 74.62.Dh

INTRODUCTION

There still exists considerable disagreement concerning the normal-state and superconducting properties of the electron-doped high-temperature superconducting cuprates (EDHTSC's). In the case of the hole doped high-temperature superconducting cuprates (HDHTSC's) it is generally agreed that the superconducting order parameter has $d_{x^2-y^2}$ symmetry,[1,2] there exists antiferromagnetic spin fluctuations,[3,4] and there also exists a normal-state pseudogap[5,6] with a similar symmetry as the superconducting gap.[7–9]

The situation is not so clear for the EDHTSC's where there is disagreement concerning the symmetry of the superconducting order parameter,[10–14] the existence and nature of the normal-state pseudogap,[15–19] and whether or not antiferromagnetic spin fluctuations exist in the EDHTSC's.[14] For example, it has been concluded from scanning superconducting quantum interference device (SQUID) microscope measurements on the EDHTSC's $Nd_{2-x}Ce_xCuO_4$ and $Pr_{2-x}Ce_xCuO_4$ that the superconducting order parameter has $d_{x^2-y^2}$ symmetry,[12] while some penetration depth[10,13] and tunneling measurements[11] on $Nd_{2-x}Ce_xCuO_4$ and $Pr_{2-x}Ce_xCuO_4$ have been interpreted in terms of a symmetry other than $d_{x^2-y^2}$ or a symmetry that changes with electronic doping. In the case of the EDHTSC $Sr_{1.9}La_{0.1}CuO_2$, tunneling data have been interpreted in terms of *s*-wave symmetry of the superconducting order parameter and the absence of antiferromagnetic spin fluctuations.[14] However, nuclear magnetic resonance (NMR) measurements on the EDHTSC $Sr_{1.9}La_{0.1}CuO_2$, have shown that the NMR data can be interpreted in terms of nodes in the superconducting gap as expected from a superconducting order parameter with $d_{x^2-y^2}$ symmetry and antiferromagnetic spin fluctuations similar to those observed in the HDHTSC's.[15,16]

It has very recently been theoretically predicted that the antiferromagnetic spin-fluctuation spectrum changes with increasing electronic doping in the EDHTSC $R_{2-x}Ce_xCuO_4$ and, similar to the HDHTSC's, a spin gap should exist in the antiferromagnetic spin-fluctuation spectrum as probed by the Cu spin-lattice relaxation data where the onset temperature is up to $\sim$1.8 times larger than the superconducting transition temperature and decreases with increasing Ce doping.[17] A gap in the electronic density of states, known as the normal-state pseudogap, has been reported in two recent tunneling studies on $Nd_{2-x}Ce_xCuO_4$ and $Pr_{2-x}Ce_xCuO_4$, but this gap only exists for temperatures less than $\sim$25 K and could only be observed by applying a magnetic field that is above the upper critical field B_{c2}. However, recent infrared reflectance measurements on $Nd_{1.85}Ce_{0.15}CuO_4$ have been interpreted in terms of a normal-state pseudogap that is large and, similar to very underdoped HDHTSC's, exists for temperatures of up to 300 K.[18] A large pseudogap has also been reported from angle-resolved photoemission spectroscopy (ARPES) measurements but these measurements were made below 20 K and in the superconducting state.[19] Interestingly, the pseudogap was reported to have a **k**-space dependence that is different from the observed in the HDHTSC's. In particular, the pseudogap is a maximum at $\mathbf{k}=(\pi,0)$ for the HDHTSC's and a maximum at the intersection of the Fermi surface with the antiferromagnetic lattice for the EDHTSC's. Therefore studies are clearly required of the Cu nuclear spin-lattice relaxation rate in the normal state of $R_{2-x}Ce_xCuO_4$ to as low a temperature as possible and for different electron doping concentrations to see if a spin gap exists or if the antiferro-

magnetic spin-fluctuation spectrum probed by the Cu spin-lattice relaxation rate changes with increasing electron doping.

In this paper we report Cu NMR measurements on the EDHTSC $Pr_{2-x}Ce_xCuO_4$ ($x=0.10$, 0.15, and 0.20) at a magnetic field that is above B_{c2} and hence enables the normal-state properties to be probed to low temperatures. Unlike the EDHTSC $Nd_{2-x}Ce_xCuO_4$ that has the same T' unit cell but different rare earth, it has been found that superconductivity exists over a wide Ce concentration range from 0.05 to 0.20 in $Pr_{2-x}Ce_xCuO_4$ and the superconducting transition temperature is nearly temperature independent.[20] We show below that the Cu NMR data can be interpreted in terms of electron doping independent antiferromagnetic spin fluctuations and there is no evidence in the Cu spin-lattice relaxation data for a large spin gap.

EXPERIMENTAL DETAILS

$Pr_{2-x}Ce_xCuO_4$ samples were made from a stoichiometric mix of Pr_6O_{11}, CeO, and CuO. The powder was pressed into pellets and then sintered in air at 1060 °C for 6 h and 1100 °C for 48 h. The sintering at 1100 °C was repeated two times with intermediate grinding. X-ray-diffraction measurements confirmed that the samples were single phase. The samples were annealed in an Ar atmosphere at 975 °C for 8 h and then rapidly quenched. This resulted in superconducting transition temperatures in zero applied magnetic field of 16 K ($x=0.10$), 20 K ($x=0.15$), and 20 K ($x=0.20$) as measured using a SQUID magnetometer. Part of the $x=0.15$ sample was also *c*-axis aligned in resin. The alignment was achieved by grinding part of the sample into a fine powder, dispersing it in a resin, and then curing it on a rotating turnstile in an applied magnetic field of 0.8 T where the applied magnetic field was perpendicular to the rotation axis. This alignment technique is necessary because $Pr_{2-x}Ce_xCuO_4$ preferentially aligns with the *ab* plane parallel to the direction of the applied magnetic field rather that with the *c* axis parallel to the direction of the applied magnetic field, which is observed in most of the other HTSC's. The dc magnetization was measured using a SQUID magnetometer and an applied magnetic field of 6 T.

Cu NMR measurements were made on *c*-axis aligned and unoriented powder samples in applied magnetic fields of 5.6, 8.45, 9, and 14.1 T. The spectra were obtained point by point using a Hahn-echo pulse sequence where the $\pi/2$ pulse width was between 2 and 10 μs and the separation between the pulses was between 30 and 40 μs. The spectra were obtained by Fourier transforming the second half of the echo and then integrating or adding the resultant spectra. The probeheads used to obtain spectra at 5.6, 8.45, and 14.1 T had a Cu background signal and hence data were not taken near the Cu background. This was not a problem for the probehead used to obtain NMR spectra and the ^{63}Cu spin lattice relaxation time $^{63}T_1$ at 9 T. The NMR shift was referenced to an aqueous CuCl suspension. Both the inversion recovery and saturating comb techniques were used to obtain $^{63}T_1$. In both cases the magnetization recovery $M(\tau)$ for the $I=\frac{3}{2}$ Cu nuclei for magnetic relaxation ($\Delta m=\pm 1$) is[21]

$$M(\tau)=M_0\left\{1-\Gamma\left[A\exp\left(-\frac{\tau}{T_1}\right)+B\exp\left(-\frac{3\tau}{T_1}\right)+C\exp\left(-\frac{6\tau}{T_1}\right)\right]\right\}, \quad (1)$$

where M_0 denotes the equilibrium magnetization and τ the time between the inversion pulse or the last saturation pulse and the detection sequence. Γ is 2 for perfect inversion and 1 for the application of a perfect $\pi/2$ saturating comb. The coefficients *A*, *B*, and *C* depend on the initial excitation conditions. For the inversion or saturation of the central $\pm\frac{1}{2}$ transition without exchange between the other levels, it can be shown that $A=0.1$, $B=0$, and $C=0.9$. In the presence of fast exchange processes these coefficients change to $A=0.4$, $B=0$, and $C=0.6$. In a previous study we found that the second scenario better fitted the Cu spin-lattice relaxation data from the EDHTSC $Sr_{0.9}La_{0.1}CuO_2$ at low temperatures.[15] As we show later, we find that *A* varies from $\sim$0.4 at low temperatures to $\sim$0.2 at high temperatures, which may indicate a change in the underlying Cu spectra from the broad Cu satellites.

RESULTS AND ANALYSIS

The ^{63}Cu NMR spectra from powder $Pr_{2-x}Ce_xCuO_4$ samples are plotted in Fig. 1(a) at 293 K and for an applied magnetic field of 9 T. The spectra contain a narrow region arising from the ^{63}Cu nuclear $+\frac{1}{2}\leftrightarrow-\frac{1}{2}$ transition that is $\sim$1.4 MHz in extent and a broad weaker region extending to $\pm$6 MHz. The resonance from the ^{65}Cu isotope (not shown) occurs at a higher frequency. Spectra taken at 5.6, 8.45, and 14.1 T are essentially the same, when scaled by the Larmor frequency, which shows that the central peak is little affected by second-order nuclear quadrupole broadening in contrast to the HDHTSC's. The weaker broad signal is also observed in the EDHTSC $Sr_{0.9}La_{0.1}CuO_2$,[15] and it is likely to be due to the $+\frac{3}{2}\leftrightarrow+\frac{1}{2}$ and $-\frac{1}{2}\leftrightarrow-\frac{3}{2}$ satellite transitions.

It is apparent in Fig. 1(a) that the width of the ^{63}Cu $+\frac{1}{2}\leftrightarrow-\frac{1}{2}$ transition at 293 K and 9 T from unaligned powder samples at room temperature is essentially the same for different Ce concentrations and the infinite CuO_2 layer EDHTSC $Sr_{0.9}La_{0.1}CuO_2$.[15] The only difference is the relative height of the peak arising from microcrystallites partially aligned with $ab\|B$. The comparable widths of the ^{63}Cu NMR central $+\frac{1}{2}\leftrightarrow-\frac{1}{2}$ transition at 293 K from $Pr_{2-x}Ce_xCuO_4$ that contains Pr^{3+} moments and $Sr_{0.9}La_{0.1}CuO_2$ that does not contain any static magnetic moments implies that the broadening of the ^{63}Cu NMR powder spectra from $Pr_{2-x}Ce_xCuO_4$ at 293 K is not significantly affected by the Pr^{3+} moment. Rather, the broadening is dominated by NMR shift anisotropy that is similar for $Pr_{2-x}Ce_xCuO_4$ and $Sr_{0.9}La_{0.1}CuO_2$.

It is evident in Fig. 1(b) that the Cu NMR spectra at room temperature from aligned $Pr_{1.85}Ce_{0.15}CuO_4$ are narrow and the spectrum for $c\|B$ occurs at a higher frequency, indicating the presence of NMR shift anisotropy. However, as the temperature is reduced there is a systematic increase in the Cu NMR linewidth as can be seen in the inset to Fig. 1(b) where

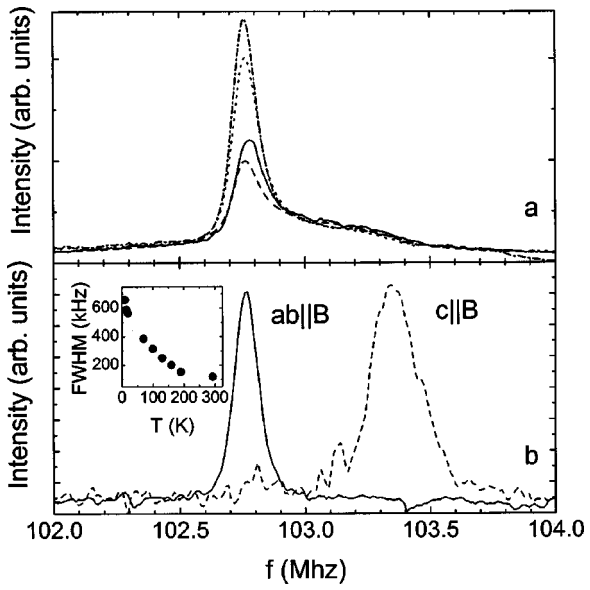

FIG. 1. (a) Plot of the ^{63}Cu NMR spectra at 293 K from a powder $Pr_{2-x}Ce_xCuO_4$ sample and an applied magnetic field of 9 T for $x=0.10$ (dotted curve), $x=0.15$ (solid curve), and $x=0.20$ (dot-dash curve). Also shown is the ^{63}Cu NMR spectrum from a powder $Sr_{0.9}La_{0.1}CuO_2$ sample (dashed curve) shifted down in frequency by 140 kHz (Ref. 15). (b) Plot of the ^{63}Cu NMR spectra at 293 K from a *c*-axis aligned $Pr_{1.85}Ce_{0.15}CuO_4$ sample and for the *c* axis parallel to the applied magnetic field (dashed curve) and the *ab* plane parallel to the applied magnetic field (solid curve). Inset: plot of the ^{63}Cu NMR linewidth against temperature for *c*-axis aligned $Pr_{1.85}Ce_{0.15}CuO_4$ with the *ab* plane parallel to the applied magnetic field of 9 T.

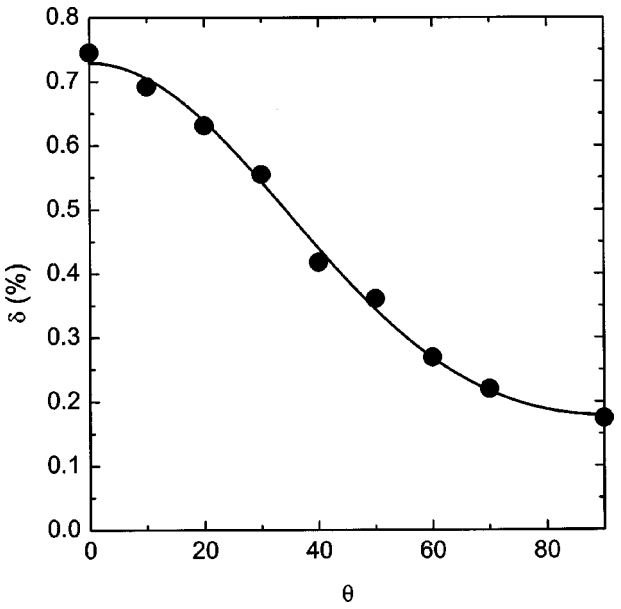

FIG. 2. Plot of the ^{63}Cu NMR shifts at 293 K and 9 T against the angle between the *c* axis and the applied magnetic field (solid circles). Also shown is a best fit to the data using Eq. (4) resulting in a ^{63}Cu NQR frequency of 4 MHz (solid curve).

the ^{63}Cu NMR linewidth is plotted for $ab\|B$. This increase is due to a static magnetic field at the Cu nucleus arising from the Pr^{3+} moment. We find no evidence for the wipe-out of the Cu NMR signal intensity in this sample or for $x=0.10$ and 0.20 that has been observed in the zero-field Cu NMR spectra from the underdoped HDHTSC $La_{2-x-y}(Eu,Nd)_y(Ba,Sr)_xCuO_4$ (Refs. 22–28) and $Y_{1-x}Ca_xBa_2Cu_3O_{7-\delta}$,[25,29] which was attributed to slowing down of the stripe dynamics or the formation of a spin glass.

The ^{63}Cu NQR frequency is an important parameter for characterizing HTSC's because it is very sensitive to the local electronic state. A previous estimate of the ^{63}Cu NQR frequency from $Pr_{1.85}Ce_{0.15}CuO_4$ was made using an indirect method resulting in a value of 1.6 MHz.[30] However, a more accurate technique involves fitting the ^{63}Cu NQR frequency as a function of the angle between the *c* axis and the applied magnetic field. For this reason, we plot in Fig. 2 the ^{63}Cu NMR shift at room temperature against the angle between the *c* axis and the applied field θ.

The ^{63}Cu NQR frequency ν_Q and the magnetic NMR shift anisotropy can be determined from Fig. 2 by noting that, for axial symmetry, the total NMR shift $\delta(\theta)$ of the central transition can be written as[31–33]

$$\delta(\theta)=\Delta\nu(\theta)/\nu_0={}^{63}K_s(\theta,T)+{}^{63}K_{\mathrm{Pr}}(\theta,T)+{}^{63}K_{\mathrm{orb}}(\theta)+\Delta\nu_q(\theta)/\nu_0, \quad (2)$$

where $\Delta\nu(\theta)$ is the shift in frequency from the Larmor frequency ν_0, $^{63}K_s(\theta,T)$ is the Knight shift arising from the conduction band carriers, $^{63}K_{\mathrm{Pr}}(\theta,T)$ is the NMR shift due to hyperfine coupling to the Pr^{3+} moment, $^{63}K_{\mathrm{orb}}(\theta)$ is the temperature independent orbital shift, and $\Delta\nu_q(\theta)/\nu_0$ is the second-order nuclear quadrupole shift. Since for Cu in the CuO_2 planes the electric-field gradient tensor with its principal components V_{xx}, V_{yy}, and V_{zz} exhibits axial symmetry, the asymmetry parameter $\eta=(V_{xx}-V_{yy})/V_{zz}$ vanishes.[32,33] Here the reference frame is chosen in a way that V_{xx} and V_{yy} are the electric-field gradients in the *a*-axis and *b*-axis directions and V_{zz} is the electric-field gradient in the *c*-axis direction. For this case, the angular dependence of the second-order quadrupole term for ^{63}Cu ($I=\frac{3}{2}$) is given by[34]

$$\Delta\nu_q(\theta)=\frac{3}{16}\frac{\nu_Q^2}{\nu_0}[9\cos^2(\theta)-1][\cos^2(\theta)-1], \quad (3)$$

where $\nu_Q=eQV_{zz}/2h$ is the nuclear quadrupole frequency with eQ denoting the nuclear quadrupole moment for ^{63}Cu. Thus the room-temperature data in Fig. 2 was fitted to

$$\delta(\theta)={}^{63}K_c\cos^2(\theta)+{}^{63}K_{ab}\sin^2(\theta)+\Delta\nu_q(\theta)/\nu_0, \quad (4)$$

where $^{63}K_c$ and $^{63}K_{ab}$ are the total magnetic shifts [first three terms in Eq. (2)] for the *c* axis parallel to the applied magnetic field and for the *ab* plane parallel to the applied magnetic field, respectively. We show by the solid curve in Fig. 2 that the best fit is obtained when $^{63}K_c=0.73\pm0.02\%$, $^{63}K_{ab}=0.15\pm0.02\%$, and $\nu_Q=4.0\pm0.8$ MHz.

The Cu NQR frequency is ~2.5 times greater than the previous estimate, but it is comparable to that estimated in the other EDHTSC, $Sr_{0.9}La_{0.1}CuO_2$ [~3 MHz (Refs. 15, 16 and 35)]. However, ν_Q is significantly less than that mea-

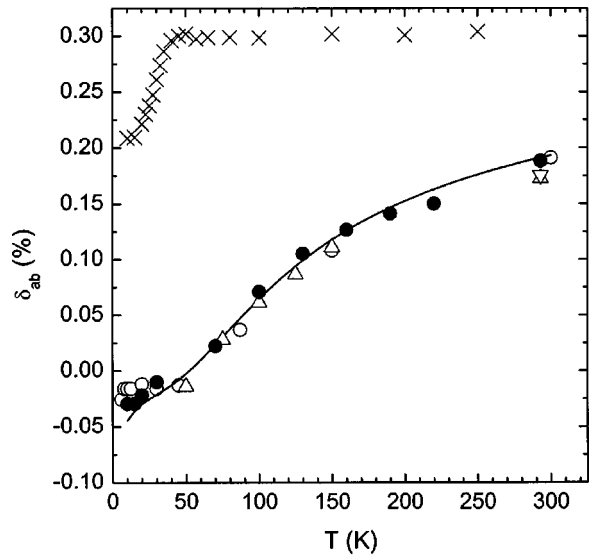

FIG. 3. Plot of the ^{63}Cu NQR shift against temperature for *c*-axis aligned $Pr_{1.85}Ce_{0.15}CuO_4$ with the *ab* plane parallel to the applied magnetic field (solid circles) and powder $Pr_{2-x}Ce_xCuO_4$ samples with $x=0.10$ (open down triangle), 0.15 (open circles), and $x=0.20$ (open up triangles). Also shown is the ^{63}Cu NMR shift from $Sr_{0.9}La_{0.1}CuO_2$ for the *ab* plane parallel to the applied magnetic field [crosses (Ref. 15)]. The solid curve is the fit to the $Pr_{2-x}Ce_xCuO_4$ data using the hyperfine coupling model described in the text and the measured susceptibility. The additional downturn at low temperatures is due to a low-temperature increase in the susceptibility. The cause of this increase has not been determined.

sured in the HDHTSC's, where ν_Q is much larger and varies from ~16 to ~40 MHz.[36] The larger ν_Q values found in the HDHTSC's have been reproduced in recent density-functional cluster calculations where the electric-field gradient (EFG) and hence ν_Q is dominated by large positive and negative contributions from various Cu $3d$ and O $2p$ orbitals.[37] We are not aware of similar calculations for the EDHTSC's, but the small ν_Q and hence small EFG at the Cu nucleus for superconducting $Pr_{1.85}Ce_{0.15}CuO_4$ and $Sr_{0.9}La_{0.1}CuO_2$ may be due to a fortuitous cancellation of the large positive a negative contributions, leading to an EFG at the Cu nucleus that is nearly zero.

It is important to know if hyperfine coupling from the Pr^{3+} moment to Cu is large in comparison to the intrinsic hyperfine coupling in the CuO_2 planes. The Pr^{3+} to Cu hyperfine coupling constant can be estimated from the temperature dependence of the Cu NMR shift data for the *ab* plane parallel to the applied magnetic field, plotted in Fig. 3. Here we plot the NMR shift for the *ab* plane parallel to the applied magnetic field from *c* axis aligned $Pr_{1.85}Ce_{0.15}CuO_4$ (filled circles), and powder $Pr_{1.90}Ce_{0.10}CuO_4$ (open down triangle), $Pr_{1.85}Ce_{0.15}CuO_4$ (open circles), and $Pr_{1.80}Ce_{0.20}CuO_4$ (open up triangles). The NMR shift for the unaligned samples was taken from the position of the peak seen in Fig. 1(a) that corresponds to grains aligned with the *ab* plane parallel to the applied magnetic field. It can be seen that the shift data all fall on a common curve. Furthermore, the NMR shifts are significantly less than those found in the EDHTSC $Sr_{0.9}La_{0.1}CuO_2$ [crosses, $T_c=43$ K (Ref. 15)], decrease with decreasing temperature, and are negative at low temperatures. Note that the NMR shift for $Sr_{0.9}La_{0.1}CuO_2$ decreases below ~43 K due to the onset of superconductivity and the decreasing density of normal-state carriers. In the case of $Pr_{2-x}Ce_xCuO_4$ the applied magnetic field is above B_{c2} and hence superconductivity is completely suppressed. The NMR shift data in Fig. 3 can be understood in terms of an additional hyperfine coupling to Pr^{3+} with a negative hyperfine coupling constant and a Knight shift, which is proportional to the spin susceptibility in the CuO_2 planes, that is essentially the same for the three different Ce concentrations.

The data in Fig. 3 were modeled by first noting that the Knight shift and the Pr^{3+} magnetic shift are proportional to the static spin susceptibility in the CuO_2 planes and the Pr^{3+} susceptibility respectively. Thus, for the *ab* plane parallel to the applied magnetic field, Eq. (2) can be written as[32]

$$^{63}K_{ab}(T)=\frac{A_{\mathrm{Cu},ab}}{g_{\mathrm{Cu,eff}}\mu_B}\frac{\chi_s^{\mathrm{molar}}}{\upsilon_{\mathrm{Cu}}N_A\mu_0}+\frac{A_{\mathrm{Cu-Pr},ab}\chi_{\mathrm{Pr}}^{\mathrm{molar}}(T)}{g_{\mathrm{Pr,eff}}\mu_B\upsilon_{\mathrm{Pr}}N_A\mu_0}+{}^{63}K_{\mathrm{orb},ab}+\frac{\Delta\nu_{q,ab}}{\nu_0}, \tag{5}$$

where $A_{\mathrm{Cu},ab}$ and $A_{\mathrm{Cu-Pr}}$ are the hyperfine coupling constants in the CuO_2 plane and from Pr^{3+} to Cu respectively. $g_{\mathrm{Cu,eff}}$ and $g_{\mathrm{Pr,eff}}$ are the effective g factors for Cu (2) and Pr^{3+} (0.8), μ_B is the Bohr magneton, χ_s^{molar} is the static molar spin susceptibility in the CuO_2 plane, and $\chi_{\mathrm{Pr}}^{\mathrm{molar}}$ is the Pr^{3+} molar susceptibility, N_A is Avagadros constant, υ_{Cu} is the number of Cu per unit cell, υ_{Pr} is the number of Pr^{3+} per unit cell, and μ_0 is the vacuum permeability. The measured susceptibility can be written as

$$\chi=\chi_{\mathrm{Cu}}+\chi_{\mathrm{Pr}}, \tag{6}$$

where χ_{Cu} is the susceptibility from the CuO_2 planes and χ_{Pr} is the Pr^{3+} susceptibility. For the HDHTSC's, χ_{Cu} is small and is less than 4×10^{-5}.[38] This is significantly less than the contribution from χ_{Pr} to the total susceptibility and hence we approximate the contribution to χ from the CuO_2 planes as a small constant term. This is not the case for the NMR shift where $A_{\mathrm{Cu},ab}$ is large [~37 T (Ref. 32)] and thus the contribution from the CuO_2 planes is significant.

We show in Fig. 3 (solid curve) that $^{63}K_{ab}$ can be modeled using Eqs. (5) and (6), the measured M/H at 6 T, and the measured temperature-independent $^{63}K_{s,ab}$ [0.09% (Ref. 15)] and $^{63}K_{s,\mathrm{orb}}$ [0.21% (Ref. 15)] in $Sr_{0.9}La_{0.1}CuO_2$, where the fitted Pr^{3+} to Cu hyperfine coupling constant is $A_{\mathrm{Pr},ab}=-0.17$ T. We find that $A_{\mathrm{Pr},ab}$ is only ~0.5% of $A_{\mathrm{Cu},ab}$.

Another important parameter is the Cu orbital shift anisotropy that depends on the splitting of the Cu $3d$ orbitals and assumptions about the occupancy of the Cu orbitals.[39,40] In the case of Cu in the CuO_2 planes of the HTSC's it has been shown that $^{63}K_{\mathrm{orb},c}/{}^{63}K_{\mathrm{orb},ab}=4E_{yz}/E_{xy}(=4E_{xz}/E_{xy})$, assuming a Cu^{2+} valence and that the hole does not extend significantly onto neighboring atoms, where E_{yz}, E_{xz}, and E_{xy} are the energies of the d_{yz}, d_{xz}, and d_{xy} orbitals, respectively, relative to the energy of the $d_{x^2-y^2}$ orbital.[39,40] The

measured orbital shift anisotropy in the HDHTSC $YBa_2Cu_3O_{7-\delta}$ is 4.54, from which it was deduced that $E_{yz}/E_{xy}=1.14$. This value is consistent with E_{yz}, E_{xz}, and E_{xy} determined from theoretical calculations[41] and experimental data,[42] where $E_{yz}=E_{xz}$ and $E_{xy}<E_{yz}$. It is not clear if the absence of an apical oxygen in $Pr_{2-x}Ce_xCuO_4$ or the larger Cu-O-Cu distance when compared with the HDHTSC's has an effect on the energies of the Cu orbitals and hence the orbital shift anisotropy. For this reason, we estimate the orbital shift anisotropy in $Pr_{2-x}Ce_xCuO_4$ by first noting that the hyperfine coupling constant in the CuO_2 planes for the *c* axis parallel to the applied magnetic field, $A_{Cu,c}$, is much smaller than $A_{Cu,ab}$ in the HDHTSC's and hence $^{63}K_c$ at room temperature is expected to be dominated by the orbital shift plus the Pr^{3+} term and hence we estimate $^{63}K_{orb,c}$ to be ~0.88%. Therefore the orbital shift anisotropy is estimated to be $^{63}K_{orb,c}/^{63}K_{orb,ab}$ ~4.2, which is slightly greater than that observed in the EDHTSC $Sr_{0.9}La_{0.1}CuO_2$ [~4.0 (Refs. 16 and 35)] and it is slightly less than that observed in the HDHTSC $YBa_2Cu_3O_{7-\delta}$ [$^{63}K_{orb,c}/^{63}K_{orb,ab}$ =4.54 (Ref. 39)]. The comparable orbital shift anisotropy in the EDHTSC's and HDHTSC's are consistent with a similar E_{yz}/E_{xy} ratio, where $E_{xy}<E_{yz}$.

While the ^{63}Cu NMR shift contains a significant hyperfine component from Pr^{3+}, we show below that the Cu spin-lattice relaxation rate is dominated by hyperfine coupling within the CuO_2 planes. We first note that the magnetization recovery from powder and aligned samples can be fitted to Eq. (1) with $A\sim0.2$, $B=0$, and $C\sim0.8$ for temperatures greater than ~50 K. However, similar to a previous study on $Pr_{1.85}Ce_{0.15}CuO_4$,[30] we find that for temperatures less than 50 K, *A* increases to ~0.4, $B=0$, and *C* decreases to ~0.6. This may be due to Pr^{3+}-induced broadening of the CU NMR spectra from the central and satellite transitions that results in a change of the initial conditions of the recovery after inversion or saturation. Additionally, the exchange rate within the Cu nuclear-spin system could increase at lower temperatures.

It should be noted that the relaxation process is governed by magnetic fluctuations over the entire temperature range measured in our study (6–300 K). This was verified by comparing the spin-lattice relaxation rates of ^{63}Cu and ^{65}Cu, where we find that ^{65}Cu has a larger spin-lattice relaxation rate. Both isotopes have a nuclear spin of $I=\frac{3}{2}$, but ^{65}Cu has a slightly larger gyromagnetic ratio and a slightly smaller quadrupole moment. Since the relaxation rate is proportional to the square of the gyromagnetic ratio for magnetic fluctuations and proportional to the square of the nuclear quadrupole moment for quadrupolar fluctuations, the observed relaxation rate enhancement for the ^{65}Cu isotope indicates a dominant magnetic relaxation mechanism.

The resultant $1/^{63}T_1T$ are plotted in Fig. 4 for powder (filled circles) and *c*-axis aligned (open circles) samples and $x=0.10$, 0.15, and 0.20. For the powder samples, $^{63}T_1$ was taken at the peak in the NMR spectra, corresponding to grains with the *ab* plane parallel to the applied magnetic field, and for the *c*-axis aligned sample, $^{63}T_1$ was taken with *ab* plane parallel to the applied magnetic field.

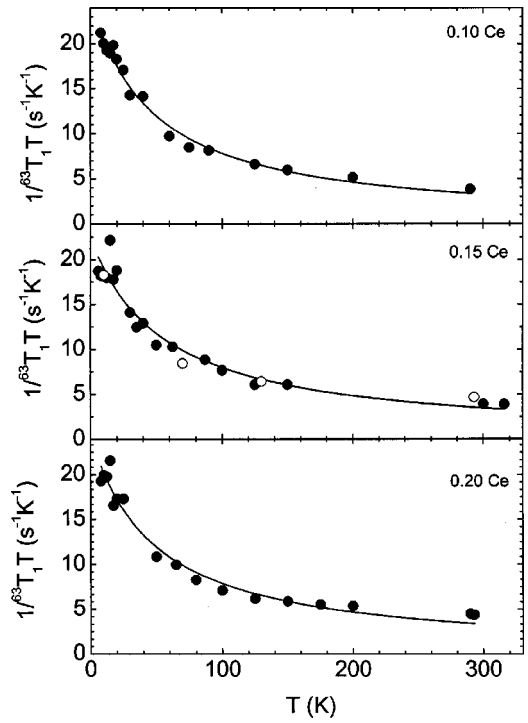

FIG. 4. Plot of $1/^{63}T_1T$ against temperature for $Pr_{2-x}Ce_xCuO_4$ powder samples (filled circles) and aligned samples with the *ab* plane parallel to the applied magnetic field (open circles) for $x=0.10$, $x=0.15$, and $x=0.20$. The solid curves are a fit to the Curie-Weiss function described in the text.

Before we discuss the spin-lattice relaxation mechanism in terms of hyperfine relaxation within the CuO_2 plane we estimate the direct spin-lattice relaxation contribution of the uncorrelated Pr^{3+} moments in a manner similar to that done for $Y_{1-x}Pr_xBa_2Cu_3O_7$ (Ref. 43) and $GdBa_2Cu_3O_7$.[44] The high temperature contribution to the Cu spin-lattice relaxation rate due to Pr^{3+} moments is given by[45]

$$T_{1,\mathrm{Pr}}^{-1}=\frac{\sqrt{2\pi}}{6}\,{}^{63}\gamma_n^2\mu_{\mathrm{Pr,eff}}^2\omega_{\mathrm{ex}}^{-1}\sum_i\frac{f(\alpha_i,\beta_i,\gamma_i)}{r_i^6}, \qquad (7)$$

where $^{63}\gamma_n$ denotes the ^{63}Cu nuclear gyromagnetic ratio, $\mu_{\mathrm{Pr,eff}}$ the effective Pr moment, ω_{ex} the Pr-Pr exchange frequency, $f(\alpha_i,\beta_i,\gamma_i)$ is a geometric factor of the order of unity depending on the direction of the lattice vector connecting the Cu nucleus and the *i*th Pr^{3+} site expressed by direction cosines $(\alpha_i,\beta_i,\gamma_i)$ with respect to the laboratory system, and r_i gives the corresponding Cu-Pr distance. Following the procedure for estimating ω_{ex} given in Refs. 43 and 44, a high-temperature limit for the relaxation process described by Eq. (7) is given by $T_{1,\mathrm{Pr}}^{-1}=100-200\ \mathrm{s}^{-1}$. At low temperatures $T_{1,\mathrm{Pr}}^{-1}$ falls below that given by Eq. 7. In our case there is an additional contribution from the van Vleck paramagnetic behavior of Pr^{3+}, which leads to a decrease in $\mu_{\mathrm{Pr},eff}$. Correcting only for this effect, which can be estimated from susceptibility measurements, we find that the direct Pr^{3+} contribution to the total ^{63}Cu spin-lattice relaxation rate is negligible over the entire temperature range

between 6 and 300 K. Therefore the ^{63}Cu spin-lattice relaxation rate $1/^{63}T_1$ is dominated by magnetic fluctuations in the CuO_2 plane.

The absolute values of $1/^{63}T_1T$, plotted in Fig. 4, are comparable to those reported in overdoped $YBa_2Cu_3O_7$ (Refs. 38 and 46) and $Y_{0.8}Ca_{0.2}Ba_2Cu_3O_7$.[47] Furthermore, $1/^{63}T_1T$ has a Curie-Weiss-like temperature dependence that is also observed in the HDHTSC's when the spin gap is small or absent. This implies the same underlying magnetic relaxation mechanism in the HDHTSC's and the EDHTSC $Pr_{2-x}Ce_xCuO_4$. In the case of the HDHTSC's, it is believed that $1/^{63}T_1T$ is dominated by antiferromagnetic spin fluctuations. The effect of antiferromagnetic spin fluctuations can be understood by noting that, when magnetic relaxation is dominant, $1/^{63}T_1T$ can be expressed as[48]

$$(^{63}T_1T)^{-1}=\frac{\hbar k_B\,{}^{63}\gamma_n^2}{2}\mathrm{Lim}_{\omega\to 0}\sum_{\mathbf{q}}|A(\mathbf{q})|\frac{\chi''(\mathbf{q},\omega)}{\hbar\omega},$$

where $|A(\mathbf{q})|$ is the form factor containing the hyperfine coupling constants and $\chi''(\mathbf{q},\omega)$ is the imaginary part of the dynamical spin susceptibility. In the Shastry, Mila, and Rice (SMR) Hamiltonian[49] that has been applied to the HTSC's, the Cu hyperfine coupling involves on-site coupling as well as nearest-neighbor Cu transferred hyperfine coupling. As a result the form factor for Cu is peaked at the antiferromagnetic wave vector $\mathbf{Q}=(\pi,\pi)$. In the presence of antiferromagnetic spin-fluctuations, where $\chi''(\mathbf{q},\omega)$ is also peaked at $\mathbf{Q}=(\pi,\pi)$, this leads to an enhancement of $1/^{63}T_1T$.

The monotonic increase in $1/^{63}T_1T$ with decreasing temperature observed in the HDHTSC's for hole concentrations were the spin gap is small is believed to arise from an increasing $\chi''(\mathbf{q},\omega)$, as weighted by the ^{63}Cu form factor and for $\omega\to 0$. Various models have been developed to account for the temperature dependence of $\chi''(\mathbf{q},\omega)$.[50–52] However, one common feature is an increase in $\chi''(\mathbf{q},\omega)$ at or near $\mathbf{Q}=(\pi,\pi)$ with decreasing temperature leading to a temperature dependence of $1/^{63}T_1T$ that is of the form $1/^{63}T_1T=(a_0T_x)/(T+T_x)$ in the absence of a spin gap or superconductivity. The appearance of a similar temperature dependence in $1/^{63}T_1T$ from $Pr_{2-x}Ce_xCuO_4$ implies, within this interpretation, that $Pr_{2-x}Ce_xCuO_4$ is also dominated by antiferromagnetic spin fluctuations. Therefore $1/^{63}T_1T$ is fitted to $1/^{63}T_1T=(a_0T_x)/(T+T_x)$ and the resultant best-fit curves are plotted in Fig. 4 (solid curves).

The fitted values of (a_0,T_x) are $(26\pm2\ \mathrm{s^{-1}\,K^{-1}},\ 44\pm4\ \mathrm{K})$, $(22\pm3\ \mathrm{s^{-1}\,K^{-1}},\ 55\pm9\ \mathrm{K})$, and $(25\pm2\ \mathrm{s^{-1}\,K^{-1}},\ 47\pm6\ \mathrm{K})$, for $x=0.10$, 0.15, and 0.20, respectively. We first note that there is no evidence of a gap in the spin-fluctuation spectrum near the antiferromagnetic wave vector in the $1/^{63}T_1T$ data that have been predicted for $R_{2-x}Ce_xCuO_4$ for temperatures down to 6 K.[17] Any spin gap should cause $1/^{63}T_1T$ to depart from the Curie-Weiss-like temperature dependence and decrease with decreasing temperature below a characteristic temperature. This result is contrary to that observed in underdoped HDHTSC's.[53]

The fitted (a_0,T_x) values are independent of electron doping within experimental uncertainty. This is inconsistent with a recent theoretical study that predicts that $1/^{63}T_1T$, and hence a_0T_x, should decrease with increasing electron doping.[17] Rather, assuming that there is no change in the hyperfine coupling constants with increased Ce concentration, the constant (a_0,T_x) values imply that there is no change in the antiferromagnetic spin-fluctuation spectrum as probed by $1/^{63}T_1T$ with increasing electronic doping from $x=0.10$ to $x=0.2$. This result can be compared with that observed in the HDHTSC $YBa_2Cu_3O_{7-\delta}$ (Refs. 38 and 46) and $Y_{0.8}Ca_{0.2}Ba_2Cu_3O_7$ (Ref. 47) at temperatures and hole concentrations where the spin gap is small. Specifically, $1/^{63}T_1T$ fits onto a common curve for $Y_{1-x}Ca_xBa_2Cu_3O_7$ where $x=0$, 0.1, and 0.2. The inclusion of data from $YBa_2Cu_3O_{7-\delta}$ where $\delta=0.08$ to 0 and using the correlation between δ and hole concentration[54] to estimate the hole concentration means that when the spin gap is small $Y_{1-x}Ca_xBa_2Cu_3O_{7-\delta}$ follows a common $1/^{63}T_1T$ for a wide hole concentration range of $\sim$0.063 holes/Cu.

Additional information about the spin dynamics in the CuO_2 planes is provided by the anisotropy of the ^{63}Cu spin-lattice relaxation rate, $^{63}R=(1/^{63}T_{1,ab})/(1/^{63}T_{1,c})$. Measurements on the HDHTSC $YBa_2Cu_3O_7$ have revealed values of ^{63}R ranging from 3.4 to 4.0,[50,55] which is significantly less than that found in antiferromagnetic CuO [$^{63}R=8$ (Ref. 16)]. The lower value of ^{63}R observed in $YBa_2Cu_3O_7$ can been accounted for by assuming the transferred hyperfine interaction, mentioned above, and antiferromagnetic spin fluctuations.[50] We find a slightly lower value of ^{63}R (2.9 ± 0.5 at 70 K) in *c*-axis aligned $Pr_{1.85}Ce_{0.15}CuO_4$ that is comparable to that measured in the infinite CuO_2 layer EDHTSC $Sr_{0.9}La_{0.1}CuO_2$ [$\sim$2.6 (Ref. 16)]. Thus ^{63}R from $Pr_{1.85}Ce_{0.15}CuO_4$ is consistent with $1/^{63}T_1T$ being dominated by coupling to antiferromagnetic fluctuations. The slightly lower value of ^{63}R observed may arise from a small change in the hyperfine coupling constants and hence different form factors.

CONCLUSION

In conclusion, we find that $1/^{63}T_1T$ from the electron-doped HTSC $Pr_{2-x}Ce_xCuO_4$ ($x=0.10$, 0.15, 0.20), is dominated by the same antiferromagnetic spin-fluctuation spectrum as that probed in the HDHTSC's at temperatures where the spin-gap effect observed in underdoped HDHTSC's is small. Similar to the overdoped and HDHTSC $Y_{1-x}Ca_xBa_2Cu_3O_{7-\delta}$ ($\sim$0.170–$\sim$0.233 holes/Cu) we find that the antiferromagnetic spin-fluctuation spectrum is independent of the number of doped carriers per Cu and there is no evidence for the theoretically predicted spin-gap effect in $1/^{63}T_1T$. These results show that $Pr_{2-x}Ce_xCuO_4$ ($x=0.10$, 0.15, 0.20), as probed by $1/^{63}T_1T$, is analogous to overdoped HDHTSC's but there is no similar change in T_c.

The orbital shift anisotropy is found to be comparable to that in the EDHTSC $Sr_{0.9}La_{0.1}CuO_2$ and the HDHTSC $YBa_2Cu_3O_{7-\delta}$ implying a similar relative spitting of the Cu E_{xy} and E_{xz} or E_{yz} orbitals. The ^{63}Cu NQR frequency is small, finite (4.0 ± 0.8 MHz), close to that estimated in the infinite layer EDHTSC $Sr_{0.9}La_{0.1}CuO_2$ ($\sim$3 MHz), but sig-

nificantly less than that in the HDHTSC's. This may be due to small changes in the individual contributions from the Cu $3d$ and O $2p$ orbitals that are similar for $Pr_{2-x}Ce_xCuO_4$ and $Sr_{0.9}La_{0.1}CuO_2$ leading to a net Cu $3d$ and O $2p$ contribution that nearly cancels the nuclei contribution to the electric-field gradient at the Cu nucleus.

ACKNOWLEDGMENTS

We acknowledge useful discussion with J. Haase and funding support from the New Zealand Marsden Fund (G.V.M.W.), the Alexander von Humboldt Foundation (G.V.M.W.), and the UK EPSRC (R.D. and A.H.).

*Present address: Grenoble High Magnetic Field Laboratory, LCMI–CNRS/MPI, 25 Avenue des Martyrs, B.P. 166, 38042 Grenoble Cedex 9, France.

[1] Z. X. Shen, W. E. Spicer, D. M. King, D. S. Dessau, and B. O. Wells, Science **267**, 343 (1995).
[2] J. R. Kirtley, C. C. Tsuei, J. Z. Sun, C. C. Chi, L.S. Yujahnes, A. Gupta, M. Rupp, and M. B. Ketchen, Nature (London) **373**, 225 (1995).
[3] J. M. Tranquada, W. J. L. Buyers, H. Chou, T. E. Mason, M. Sato, S. Shamoto, and G. Shirane, Phys. Rev. Lett. **64**, 800 (1990).
[4] G. Shirane, R. J. Birgeneau, Y. Endoh, P. Gehring, M. A. Kastner, K. Kitazawa, H. Kojima, I. Tanaka, T. R. Thurston, and K. Yamada, Phys. Rev. Lett. **63**, 330 (1989).
[5] W. W. Warren, R. E. Walstedt, G. F. Brennert, R. J. Cava, R. Tycko, R. F. Bell, and G. Dabbagh, Phys. Rev. Lett. **62**, 1193 (1989).
[6] H. Alloul, P. Mendels, H. Casalta, J. F. Marucco, and J. Arabski, Phys. Rev. Lett. **67**, 3140 (1991).
[7] A. G. Loeser, Z. X. Zhen, D. S. Dessau, D. S. Marshall, C. H. Park, P. Fournier, and A. Kapitulnik, Science **273**, 325 (1996).
[8] H. Ding, Y. Yokoya, J. C. Campuzano, T. Takahashi, M. Randeria, M. R. Norman, T. Mochiku, K. Kadpwski, and J. Giapintzakis, Nature (London) **382**, 51 (1996).
[9] G. V. M. Williams, J. L. Tallon, E. M. Haines, R. Michalak, and R. Dupree, Phys. Rev. Lett. **78**, 721 (1997).
[10] J. A. Skinta, M. S. Kim, T. R. Lemberger, T. Greibe, and M. Naito, Phys. Rev. Lett. **88**, 207005 (2002).
[11] J. A. Skinta, T. R. Lemberger, T. Greibe, and M. Naito, Phys. Rev. Lett. **88**, 207003 (2002).
[12] C. C. Tsuei and J. R. Kirtley, Phys. Rev. Lett. **85**, 182 (2000).
[13] A. Biswas, P. Fournier, M. M. Qazibash, V. M. Smolyaninova, H. Balci, and R. L. Greene, Phys. Rev. Lett. **88**, 207004 (2002).
[14] C. T. Chen, P. Seneor, N. C. Yeh, R. P. Vasquez, L. D. Bell, C. U. Jung, J. Y. Kim, M. S. Park, H. J. Kim, and S. I. Lee, Phys. Rev. Lett. **88**, 227002 (2002).
[15] G. V. M. Williams, R. Dupree, A. Howes, S. Krämer, H. J. Trodahl, C. U. Jung, Min-Seok Park, and Sung-Ik Lee, Phys. Rev. B **65**, 224520 (2002).
[16] T. Imai, C. P. Slichter, J. L. Cobb, and J. T. Markert, J. Phys. Chem. Solids **56**, 1921 (1995).
[17] A. Kobayashi, A. Tsuruta, T. Matsuura, and Y. Kuroda, J. Phys. Soc. Jpn. **71**, 1640 (2002).
[18] E. J. Singley, D. N. Basov, K. Kurahashi, T. Uefuji, and K. Yamada, Phys. Rev. B **64**, 224503 (2001).
[19] N. P. Armitage, D. H. Lu, C. Kim, A. Damascelli, K. M. Shen, F. Ronning, D. L. Feng, P. Bogdanov, Z.-X. Shen, Y. Onose, Y. Taguchi, Y. Tokura, P. K. Mang, N. Kaneko, and M. Greven, Phys. Rev. Lett. **87**, 147003 (2001).
[20] M. Brinkmann, T. Rex, H. Bach, and K. Westerholt, Phys. Rev. Lett. **74**, 4927 (1995).
[21] E. R. Andrew and D. P. Tunstall, Proc. R. Soc. London **78**, 1 (1961).
[22] A. W. Hunt, P. M. Singer, K. R. Thurber, and T. Imai, Phys. Rev. Lett. **82**, 4300 (1999).
[23] G. B. Teitelbaum, I. M. Abu-Shiekah, O. Bakharev, H. B. Brom, and J. Zaanen, Phys. Rev. B **63**, 020507 (2000).
[24] N. J. Curro, P. C. Hammel, B. J. Suh, M. Hücker, B. Bücher, U. Ammerahl, and A. Revcolevschi, Phys. Rev. Lett. **85**, 642 (2000).
[25] P. M. Singer and T. Imai, Phys. Rev. Lett. **88**, 187601 (2002).
[26] M. H. Julien, A. Campana, A. Rigamonti, P. Carretta, F. Borsa, P. Kuhns, A. P. Reyes, W. G. Moulton, M. Horvatić, C. Berthier, A. Vietkin, and A. Revcolevschi, Phys. Rev. B **63**, 144508 (2001).
[27] T. Sawa, M. Matsumura, and H. Yamagata, J. Phys. Soc. Jpn. **70**, 3503 (2001).
[28] M. Matsumura, T. Ikeda, and H. Yamagata, J. Phys. Soc. Jpn. **69**, 1023 (2000).
[29] Y. Kobayashi, T. Miyashita, M. Ambai, T. Fukamachi, and M. Sato, J. Phys. Soc. Jpn. **70**, 1133 (2001).
[30] A. N. Bakharev, A. G. Volodin, A. V. Duglav, A. V. Egorov, M. V. Eremin, A. Yu. Zavidonov, O. V. Lazina, M. S. Tagirov, and M. A. Teplov, Zh. Eksp. Teor. Fiz. **101**, 693 (1992) [Sov. Phys. JETP **74**, 370 (1992).
[31] C. P. Slichter, *Principles of Magnetic Resonance*, 3rd ed. (Springer, New York, 1990).
[32] M. Mehring, Appl. Magn. Reson. **3**, 383 (1992).
[33] C. Berthier, M. H. Julien, M. Horvatić, and Y. Berthier, J. Phys. I **6**, 2205 (1996).
[34] D. Freude and J. Haase, in *NMR Basic Principles and Progress*, Vol. 29 (Springer, Berlin, 1993), p. 1.
[35] K. Mikalev, K. Kumagai, Y. Furukawa, V. Bobrovski, T. D'yachkova, N. Kad'irova, and A. Gerashenko, Physica C **304**, 165 (1998).
[36] For a review, see K. Asayama, Y. Kitaoka, G. Q. Zheng, and K. Ishida, Prog. Nucl. Magn. Reson. Spectrosc. **28**, 221 (1996).
[37] S. Pliberšek and P. F. Meier, Europhys. Lett. **50**, 789 (2000).
[38] M. Takigawa, A. P. Reyes, P. C. Hammel, J. D. Thompson, R. H. Heffner, Z. Fisk, and K. C. Ott, Phys. Rev. B **43**, 247 (1991).
[39] S. E. Barrett, D. J. Durand, C. H. Pennington, C. P. Slichter, T. A. Friedmann, J. P. Rice, and D. M. Ginsberg, Phys. Rev. B **41**, 6283 (1990).
[40] C. H. Pennington, D. J. Durand, C. P. Slichter, J. P. Rice, E. D. Bukowski, and D. M. Ginsberg, Phys. Rev. B **39**, 2902 (1989).
[41] A. K. McMahan, R. M. Martin, and S. Satpathy, Phys. Rev. B **38**, 6650 (1998).
[42] J. A. Leiro, F. Werfel, and G. Dräger, Phys. Rev. B **44**, 7718 (1991).
[43] A. P. Reyes, D. E. MacLaughlin, M. Takigawa, P. C. Hammel, R. H. Heffner, J. D. Thompson, and J. E. Crow, Phys. Rev. B **43**, 2989 (1991).

[44] P. C. Hammel, M. Takigawa, R. H. Heffner, and Z. Fisk, Phys. Rev. B **38**, 2832 (1988).
[45] T. Moriya, Prog. Theor. Phys. **16**, 23 (1956).
[46] C. Berthier, M.-H. Julien, O. Bakarev, M. Horvatić, and P. Ségransan, Physica C **282-287**, 227 (1997).
[47] G. V. M. Williams and S. Krämer, Phys. Rev. B **64**, 104506 (2001).
[48] T. Moriya, J. Phys. Soc. Jpn. **18**, 516 (1963).
[49] B. S. Shastry, Phys. Rev. Lett. **63**, 1288 (1989); F. Mila and T. M. Rice, Physica C **157**, 561 (1989).
[50] A. J. Millis, H. Monien, and D. Pines, Phys. Rev. B **42**, 167 (1990).
[51] P. Carretta, A. Rigamonti, and R. Sala, Phys. Rev. B **55**, 3734 (1997).
[52] T. Moriya and K. Ueda, Adv. Phys. **49**, 555 (2000).
[53] W. W. Warren, R. E. Walstedt, G. F. Brennert, R. J. Cava, R. Tycko, R. F. Bell, and G. Dabbagh, Phys. Rev. Lett. **62**, 1193 (1989); M. Horvatić, P. Ségransan, C. Berthier, Y. Berthier, P. Butaud, J. Y. Heng, M. Couach, and J. P. Chaminade, Phys. Rev. B **39**, 7332 (1989).
[54] J. L. Tallon, C. Bernhard, H. Shaked, R. L. Hitterman, and J. D. Jorgensen, Phys. Rev. B **51**, 12 911 (1995).
[55] S. E. Barrett, J. A. Martindale, D. J. Durand, C. H. Pennington, C. P. Slichter, T. A. Friedmann, J. P. Rice, and D. M. Ginsberg, Phys. Rev. Lett. **66**, 108 (1991).